

Received: 2016.03.16  
Accepted: 2016.05.30  
Published: 2017.01.17

# The Mechanism of Computed Tomography-Guided <sup>125</sup>I Particle in Treating Lung Cancer

Authors' Contribution:  
Study Design A  
Data Collection B  
Statistical Analysis C  
Data Interpretation D  
Manuscript Preparation E  
Literature Search F  
Funds Collection G

**BF 1 Jianzhong Cheng**  
**CD 1 Shaozeng Ma**  
**CG 2 Guanghua Yang**  
**AD 2 Lisen Wang**  
**AE 1 Wei Hou**

1 Department of Ultrasound, Zhumadian Central Hospital, Zhumadian, Henan, P.R. China  
2 Department of Internal Medicine, Zhumadian Central Hospital, Zhumadian, Henan, P.R. China

**Corresponding Author:** Wei Hou, e-mial: [houweitt@sina.com](mailto:houweitt@sina.com)

**Source of support:** Departmental sources

**Background:** The incidence of malignant tumor has gradually increased. How to improve the survival and quality of life of patients who lose the opportunity for surgery or who are unwilling to receive surgery remains an obstacle. At present, <sup>125</sup>I particle interstitial implant therapy has been applied in a variety of treatments of tumors. However, the mechanism of computed tomography (CT)-guided <sup>125</sup>I particle therapy in lung cancer has not been fully elucidated.





**Material/Methods:** A total of 42 patients with advanced non-small cell lung cancer were retrospectively analyzed between January 2013 and December 2013, including 19 patients who received CT-guided <sup>125</sup>I particle therapy and 23 patients who received chemotherapy. Curative effect and adverse reactions at 6 months and 12 months were compared and analyzed. A rabbit lung cancer VX2 model was treated by <sup>125</sup>I particle implantation therapy under CT guidance. The change in tumor volume was detected. Tumor cell apoptosis was tested by flow cytometry. Bcl-2 and Bax expression were determined by real-time polymerase chain reaction (PCR) and Western blot.

**Results:** <sup>125</sup>I particle therapy obviously reduced tumor volume after 6 months and 12 months. It showed significantly higher efficiency (57.9%, 57.9%) and control (78.9%, 73.7%) than the rates of efficiency and control in the chemotherapy group (P<0.05). <sup>125</sup>I particle implantation therapy markedly suppressed rabbit VX2 transplanted tumor cell proliferation, promoted tumor regression, induced tumor cell apoptosis, reduced Bcl-2 expression, and upregulated Bax expression level (P<0.05).

**Conclusions:** CT-guided <sup>125</sup>I particle implantation therapy can inhibit tumor proliferation and growth by regulating the expression of apoptosis-related genes and proteins, which is a promising approach in lung cancer treatment.

**MeSH Keywords:** **Adrenal Gland Neoplasms • Apoptosis Inducing Factor • Genes, Intracisternal A-Particle**

**Full-text PDF:** <http://www.medscimonit.com/abstract/index/idArt/898526>

 2546  6  6  27



## Background

The incidence of malignant tumor keeps on increasing, while the fatality rate stays at a high level. Tumor prevention, treatment, and prognosis receive wide attention [1,2]. For some cancer patients who cannot tolerate surgery or whose disease is beyond surgical indications, reasonable treatment is of great need to improve quality of life and personal survival [3,4]. Tumor comprehensive treatment, including surgery, radiotherapy, chemotherapy, and other methods, is based on the patient's condition and clinical staging [5,6].

Interstitial brachytherapy was not commonly used in clinic at first because of its inaccurate positioning and poor protection system [7,8]. However, the application of a new type of radioactive <sup>125</sup>I particle, combined with computed tomography (CT) guidance, presents the benefits of precise positioning, a three-dimensional treatment plan, and a quality authentication system, and promotes the development of radioactive particle technique in tumor therapy [9,10]. Compared with conventional external radiotherapy, interstitial brachytherapy features fewer complications, less trauma, safety, and efficacy. It further improves the anti-tumor effect via killing tumor cells and most effectively protects normal tissue [11,12], and therefore has been rapidly applied in clinic. At present, the preferred choice of therapy in early prostate cancer therapy is interstitial implant with <sup>125</sup>I particle. It also showed a beneficial curative effect in the treatment of gynecologic cancers and was gradually applied in the treatment of liver cancer, pancreatic cancer, digestive tract cancer, lung cancer, and central nervous system tumor [13–16]. Nevertheless, the mechanism of CT-guided <sup>125</sup>I particles in the treatment of lung cancer has not yet been fully elucidated. In this article, we retrospectively observed CT-guided <sup>125</sup>I particles in the medical treatment of advanced lung cancer in patients, and established a rabbit VX2 tumor model to analyze its specific mechanism [17].

## Material and Methods

### Object of study

A total of 42 patients with non-small cell lung cancer (NSCLC) in Zhumadian Central Hospital (Zhumadian, Henan, China) between January 2013 and December 2013 were selected, including 19 patients who received CT-guided <sup>125</sup>I particle therapy (<sup>125</sup>I particle group) and 23 patients who received chemotherapy (chemotherapy group). All the enrolled subjects had clinic (cough, hemoptysis, pectoralgia, and dyspnea), pathology (squamous-cell carcinoma or adenocarcinoma), sputum cytology, and iconography diagnosis. All these patients were at stage III or IV according to American Joint Committee on Cancer (AJCC) TNM staging system for lung cancer (6th edition, 2002). There were 25 males and 17

females with average age of 58.4±11.2 years (range: 35–78 years). Pathological histology type included 22 cases of squamous carcinoma and 20 cases of adenocarcinoma. The two groups showed no statistical differences in general clinical information (Table 1).

The study protocol was approved by the Research Ethics Committee of Zhumadian Central Hospital, and all patients gave their informed consent before study commencement.

### Experimental animals

New Zealand rabbits aged 3–4 months and weighing 2–3 kg (range: 2.5±0.32 kg) were provided by the experimental animal center in Zhengzhou University. The rabbits were fed in a specific pathogen-free (SPF) animal house.

Rabbits were used for all experiments, and all procedures were approved by the Animal Ethics Committee of Zhumadian Central Hospital.

### Main materials and instruments

Surgical instruments were bought from the Suzhou medical instrument factory. The operating microscope was purchased from Zhenjiang Optical Instrument Co., Ltd. The VX2 rabbit tumor transplantation cell line was obtained from the Beijing Cancer Institute (Beijing, China). Trizol reagent was from Invitrogen (Carlsbad, California, USA). The polyvinylidene difluoride (PVDF) membrane was from Pall Life Sciences (Port Washington, New York, USA). Western blot-related chemical reagents were from Beyotime (Shanghai, China). The enhanced chemiluminescence (ECL) reagent was from Amersham Biosciences (Piscataway, New Jersey, USA). Bcl-2 and Bax primary antibodies, and horseradish peroxidase (HRP) tagged immunoglobulin G (IgG) secondary antibody were from Cell Signaling Technology (Danvers, Massachusetts, USA). The RNA extraction kit, reverse transcription kit, and Annexin V-FITC apoptosis detection kit were from BD Biosciences (San Jose, California, USA). The microplate reader was obtained from BD Biosciences. The DNA amplifier was from PE Gene Amp PCR System 2400. FACS Calibur flow cytometry was from BD Biosciences. Other common reagents were purchased from Sangon (Shanghai, China). The <sup>125</sup>I particle group received <sup>125</sup>I with surface activity at 0.6–1.0 mCi and a half-life of 59.21 d. It mainly emitted X-rays and γ rays. The treatment planning system (TPS), implanted devices, and protection system were bought from Beijing Senke Technology Co., Ltd. (Beijing, China).

### Methods

#### *Therapeutic schedule for NSCLC patients*

The patients in the chemotherapy group received paclitaxel (Harbin Pharmaceutical Co., Ltd., Harbin, China) and cisplatin

**Table 1.** General information comparison.

Index	<sup>125</sup> I particle	Chemotherapy
Cases (n)	19	23
Gender (Male/Female)	11/8	14/9
Age (year)	59±10.8	57.6±12.3
Histology type (squamous/adenocarcinoma)	10/9	12/11
Stage (III/IV)	7/12	10/13

(Qilu Pharmaceutical Co., Ltd, Jinan, China) combination chemotherapy with 28 days for a cycle and a total of four cycles. Support therapy including anti-nausea medication and liver protection was used during chemotherapy. <sup>125</sup>I particle implantation was done in patients in the <sup>125</sup>I particle group by using CT (GE MAX640) guided percutaneous puncture. Particle dose in the tumor target lesion and its surrounding space was determined based on the TPS and CT image. The total volume of each tumor was calculated according to CT image with the TPS before implantation. CT was used to confirm the puncture location and the implant. Information from CT or magnetic resonance imaging (MRI) images was reconstructed into a three-dimensional form, and the precise margin of the tumor was outlined to facilitate the calculation of tumor-matched peripheral dose. The TPS system was used to evaluate dose and puncture quality. Routine support treatment such as anti-inflammation and hemostasis was adopted.

#### Observational index

Tumor volume changes were assessed based on imaging to analyze the curative effect. Efficacy evaluation was performed according to the World Health Organization (WHO) tumor lesion classification and curative effect evaluation, including complete remission (CR), partial response (PR), no change (NC), and progress (PD). Effective rate means the percentage of CR and PR. Control rate means the percentage of CR, PR, and NC.

#### Rabbit VX2 tumor modeling and <sup>125</sup>I particle treatment

Experimental animals were used in the model after one week's adaptive breeding. General anesthesia was performed using 3% pentobarbital sodium 1 mL/kg ear intravenous injection. Then the rabbit received thoracotomy and CT scan to select and determine the surgical site. After assessing puncture depth and angle, the sheath of an 18 G needle was put into the tissue using the sandwich method. (At the predetermined position, pull out the needle core and put 2-3 blocks of tumor tissue into the needle sheath using ophthalmological forceps clip, followed by moving the tumor tissue blocks in using the core of the puncture needle.) The puncture needle was pierced

into lung tissue based on CT guidance and 1 mL of cells was injected. Antibiotics (0.5 g of cephalosporin muscle injection) were used to prevent infection. CT scan and X-ray confirmed that the tumor preparation was successful after 4 weeks. Then the rabbits were randomly divided into two groups. <sup>125</sup>I particle with initial activity at 0.8 mCi was put into an 18 G puncture needle. Then the particle was emitted to the site according to the TPS plan and under CT guidance [18].

#### General state observation

General state was observed before and after treatment, including mental status, appetite, and activity. Rabbit weight was recorded before <sup>125</sup>I particle implantation, 2 weeks after treatment, and 4 weeks after treatment.

#### Sample collection

A blood sample was collected from the portal vein at 2 weeks and 4 weeks after treatment, and centrifuged at 3000 rpm for 15 min. The serum was put into an Eppendorf tube and placed in a refrigerator at -20°C. Tumor tissue was collected from rabbits after they were euthanized by using ketamine/xylazine and ether, and preserved in liquid nitrogen.

#### Flow cytometry

Tumor tissue was centrifuged at 1500 revolutions per minute (r/min) for 5 min and filtrated to a precooled tube. Tumor cell suspension was placed in Dulbecco's Modified Eagle's Medium (DMEM) containing 10% fetal bovine serum (FBS) and seeded in a 96-well plate at 5×10<sup>3</sup> cells for 24 h. Then the cells were collected at 2×10<sup>6</sup> and washed with phosphate-buffered saline (PBS). After centrifugation at 1000 rpm for 5 min, the cells were fixed in precooled 75% ethanol at 4°C overnight. After washing with PBS, the cells were resuspended in 800 μL of PBS containing 1% bovine serum albumin (BSA), 100 μL of propidium iodide (PI) solution (3.8% sodium citrate, pH 7.0), and 100 μL of RnaseA (10 mg/mL). After incubation at 37°C and avoidance of light for 30 min, the cells were tested using flow cytometry and analyzed by FCSEXPRESS 3.0 software.

**Table 2.** Primer sequence.

Gene	Forward	Reverse
GADPH	ACCAGGTATCTGCTGGTTG	TAACCATGATGTCAGCGTGT
Bcl-2	TAGCAGCTTATGTCTACTGGAC	TTCTCAAGTTTCTTACCGCTA
Bax	TGCATGCTTCTGATGCCATAG	CTTCGCTTCGTCAACTCTTATC

**Table 3.** NSCLC patient tumor volume comparison (mm<sup>3</sup>).

	Before treatment	6 months	12 months
<sup>125</sup> I particle (n=19)	5.2±1.1	2.1±0.7*#	2.6±0.8*#
Chemotherapy (n=23)	5.1±1.3	3.1±0.9*	3.8±0.6*

\*  $P < 0.05$ , compared with before treatment; #  $P < 0.05$ , compared with chemotherapy.

**Table 4.** NSCLC patient curative effect comparison.

	6 months						12 months					
	CR	PR	NC	PD	Control rate (%)	Effective rate (%)	CR	PR	NC	PD	Control rate (%)	Effective rate (%)
<sup>125</sup> I particle	3	8	4	4	78.9	57.9*	2	5	7	5	73.7	36.8*
Chemotherapy	1	5	8	9	60.8	26.1	0	4	6	13	43.5	17.4

\*  $P < 0.05$ , compared with chemotherapy.

### Real-time polymerase chain reaction (PCR)

Total RNA was extracted by Trizol according to the manual and reverse transcribed to cDNA. Primers used were designed by Primer 6.0 and synthesized by Invitrogen (Table 2). Real time PCR was performed based on the following conditions: 55°C for 1 min, followed by 35 cycles of 92°C for 30 s, 5°C for 45 s, and 72°C for 35 s. GAPDH was selected as reference. Relative expression level was calculated by the 2<sup>-ΔΔCt</sup> method.

### Western blot

Lung tissue was ground in liquid nitrogen and treated with RIPA for 15–30 min. Then the tissue was ultrasonicated at 5 s × 4 times and centrifuged at 4°C and 10,000×g for 15 min. The supernatant was stored at -20 °C. The protein was separated by 10% sodium dodecyl sulfate-polyacrylamide gel electrophoresis (SDS-PAGE) and transferred to PVDF membrane. After block by 5% skim milk for 2 h, the membrane was incubated in primary antibody (1:1000) at 4°C overnight. Next, the membrane was further incubated in secondary antibody (1:2000) at room temperature for 30 min after washing with phosphate-buffered saline/Tween (PBST). At last, the membrane was mixed with chemiluminescent agent for 1 min and developed. Protein image processing system software and

Quantity One software were adopted for scanning and calculation. All the experiments were repeated four times (n=4).

### Statistical analysis

SPSS 19.0 was used for data analysis. Measurement data are presented as mean ± standard deviation and were compared by using the t-test. Enumeration data are presented as percentages and were compared by using the chi-square test.  $P < 0.05$  was considered as statistical significance.

## Results

### Curative effect comparison

After 6 months and 12 months of treatment, the curative effects in the two groups were compared. It was shown that both chemotherapy and <sup>125</sup>I particle implantation significantly reduced tumor volume, increasing both the effective rate and the control rate ( $P < 0.05$ ). Patients receiving CT-guided <sup>125</sup>I particle implantation had more obvious reduction of tumor volume and a significant rise of the effective rate and the control rate compared with the rates in the chemotherapy group ( $P < 0.05$ ) (Tables 3, 4).

**Table 5.** <sup>125</sup>I particle implantation impact on rabbit VX2 tumor transplantation model weight (kg).

Group	0 day	2 weeks	4 weeks
Test	2.53±0.97	2.09±0.62	1.76±0.92
Control	2.48±1.09	2.21±0.91	2.13±0.89*

\* P<0.05, compared with control.

**Table 6.** <sup>125</sup>I particle implantation impact on rabbit VX2 tumor transplantation model tumor volume (mm<sup>3</sup>).

Group	0 day	2 weeks	4 weeks
Control	81.26±7.17	178.37±18.23	342.68±18.92
1.0 mCi <sup>125</sup> I	82.76±8.23	158.81±1.56	211.21±23.28*

\* P<0.05, compared with control.

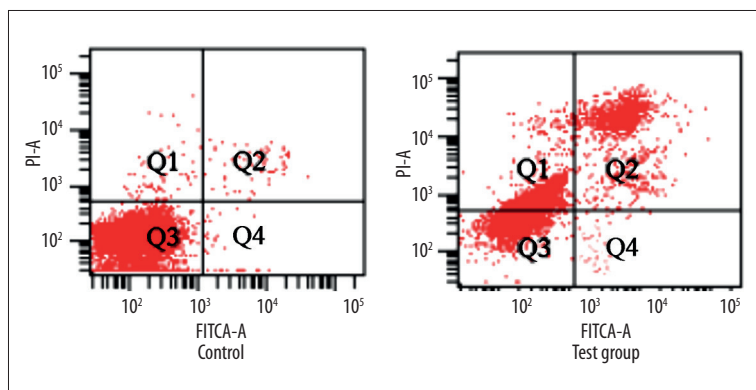


**Figure 1.** The impact of <sup>125</sup>I particle implantation on tumor cell apoptosis in the rabbit VX2 tumor transplantation model.

**Survival state comparison**

The success rate of rabbit tumor transplantation was 100%. The behavior of rabbits in the two groups after modeling was similar, including depression, activity reduction, loss of appetite, hair gloss reduction, and even unhairing. Some rabbits presented pleura plantation or transfer, and dyspnea was aggravated with the time elapsed. No rabbit died until the end of the experiment. After <sup>125</sup>I particle implantation treatment, the survival condition of the rabbits improved, with better spirit, activity, response, and appetite than the control rabbits (Table 5).

**<sup>125</sup>I particle implantation impact on tumor volume**

CT scan was performed at 2 weeks and 4 weeks after treatment to calculate tumor volume. Tumor volume at 2 weeks after treatment in each group was similar to that before treatment (P>0.05). At 4 weeks after treatment, tumor volume in the control group kept on increasing; by contrast, the degree of increase in the treated group was markedly smaller (P<0.05) (Table 6).

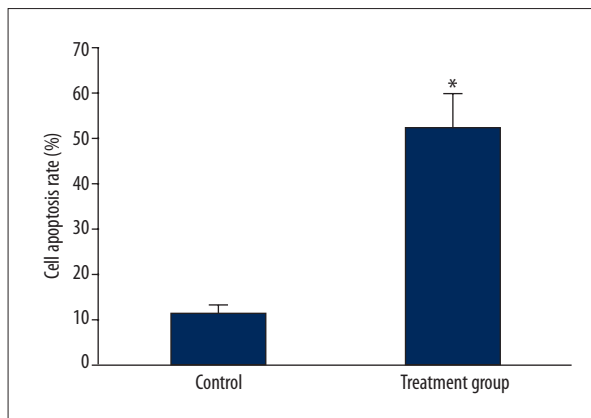


**Figure 2.** Analysis of the impact of <sup>125</sup>I particle implantation on tumor cell apoptosis in the rabbit VX2 tumor transplantation model. \* P<0.05 compared with control.

**<sup>125</sup>I particle implantation impact on tumor cell apoptosis**

Tumor cell suspension was prepared from tumor tissue. Flow cytometry was applied to detect tumor cell apoptosis. Cell apoptotic rate in the rabbit VX2 tumor transplantation model with <sup>125</sup>I particle implantation treatment for 4 weeks obviously increased (P<0.05) (Figures 1, 2).

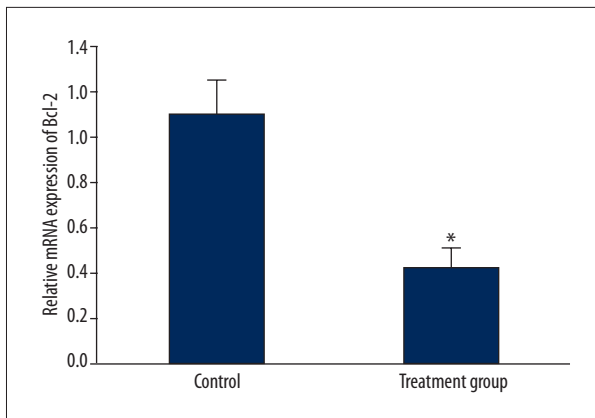


**Figure 3.** The impact of <sup>125</sup>I particle implantation on Bcl-2 mRNA expression in the rabbit VX2 tumor transplantation model. \*  $P < 0.05$ , compared with control.

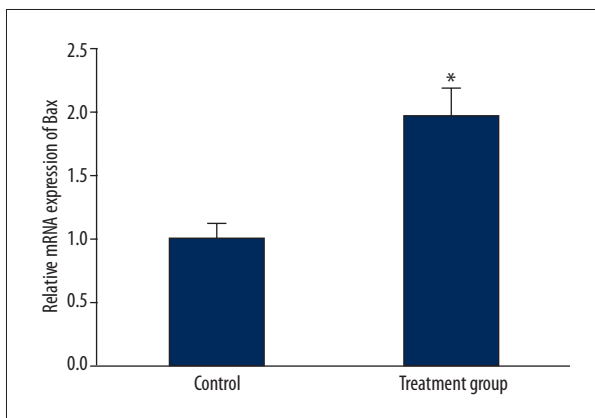


**Figure 4.** The impact of <sup>125</sup>I particle implantation on Bax mRNA expression in the rabbit VX2 tumor transplantation model. \*  $P < 0.05$  compared with control.

#### <sup>125</sup>I particle implantation impact on Bcl-2 and Bax mRNA expression in tumor tissue

Real-time PCR was performed to detect expression changes of Bcl-2 and Bax mRNA in tumor tissue. The results showed that Bcl-2 mRNA in the treatment group obviously declined compared with that in the control group ( $P < 0.05$ ) (Figure 3). Contrary to Bcl-2 mRNA, Bax mRNA was overexpressed in the treatment group compared with the control group ( $P < 0.05$ ) (Figure 4).

#### <sup>125</sup>I particle implantation impact on Bcl-2 and Bax protein expression in tumor tissue

Western blot was used to test Bcl-2 and Bax protein expression in tumor tissue. Similar to the expressions of Bcl-2 and Bax mRNA, Bcl-2 protein in the treatment group was obviously reduced compared with that in the control group ( $P < 0.05$ ) (Figure 5). Conversely, the level of Bax protein was upregulated in the treatment group compared with the control group ( $P < 0.05$ ) (Figure 6).

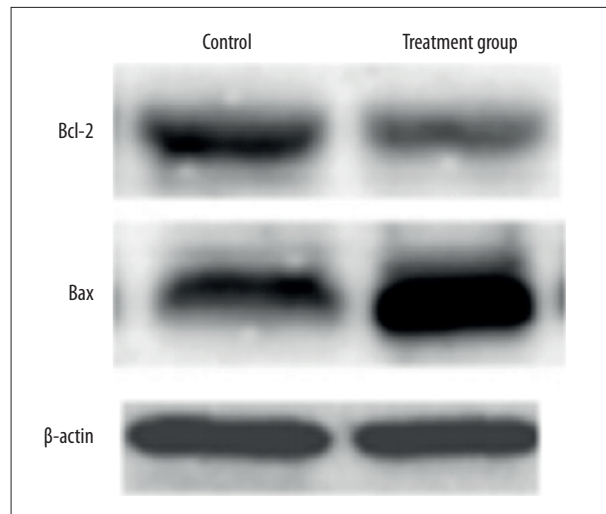


**Figure 5.** The impact of <sup>125</sup>I particle implantation on protein levels of Bcl-2 and Bax in the rabbit VX2 tumor transplantation model.

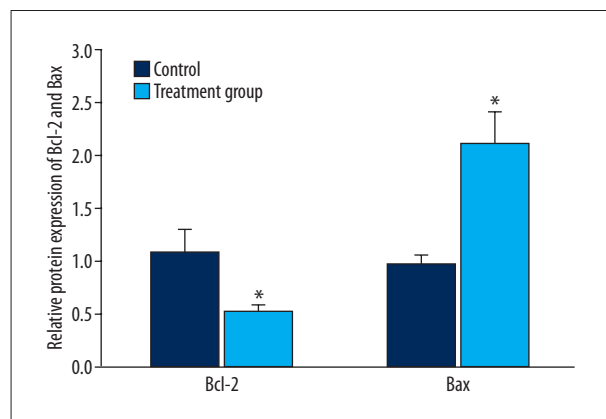


**Figure 6.** Analysis of the impact of <sup>125</sup>I particle implantation on Bax protein expression. \*  $P < 0.05$ , compared with control.

## Discussion

In recent years, it has been demonstrated that the new <sup>125</sup>I particle is characterized by low radioactivity, small trauma to normal tissue, high efficacy, precise accuracy, etc. On the basis of the development of ultrasound, CT, MRI, imaging technology, and computer 3D treatment, interstitial implantation combined with close-distance radiation therapy exhibited better therapeutic value and resulted in better patient vitality. The CT-guided positioning system enables the new type of <sup>125</sup>I radioactive particle to have more extensive application prospects in tumor treatment [19,20]. NSCLC is a common malignant tumor with an increasing incidence and mortality rate year by year. Advanced NSCLC is difficult to cure, leading to patients' survival and quality of life declining seriously [21,22]. Due to its aggregation in the target area with low radiation to

the surrounding normal tissue and the profile of quick attenuation of radiation, <sup>125</sup>I radioactive particle is recognized as a potent tool in lung cancer treatment. CT guidance can obviously reduce operating time and radiation dose, and elevate puncture accuracy, resulting in small trauma, apparent curative effect, rapid recovery, and fewer adverse reactions [23,24]. This study retrospectively compared the effect of CT-guided <sup>125</sup>I radioactive particles and chemotherapy in the treatment of NSCLC. The results revealed that patients receiving <sup>125</sup>I particle therapy had significantly smaller tumor volume, a better effective rate, and a better control rate.

We further investigated the mechanism of <sup>125</sup>I particle in treating lung cancer by establishing and using an animal VX2 transplant tumor model. The results confirmed that <sup>125</sup>I particle treatment induced tumor cell apoptosis, with decreasing Bcl-2 level and growing Bax expression, thus reducing tumor volume and improving the quality of animal survival. The occurrence and development of tumor are to some extent responsible for the imbalance of apoptosis and anti-apoptosis, among which Bcl-2 and Bax, as the member of the Bcl-2 family, draw more attention. This is because Bcl-2 mainly plays an inhibitory role in cell apoptosis and is often found overexpressed in various

tumors [25]. Bax, however, shows a negative correlation with the Bcl-2 effect, acting as a pro-apoptotic protein released from mitochondria, such as cytochrome C. It further activates caspase-3 protease, facilitates reactive oxygen generation, promotes nucleus fragmentation, and damages cell membrane to induce apoptosis and maintain normal cell proliferation [26,27].

## Conclusions

Our data demonstrated that <sup>125</sup>I particle targeted therapy had more accurate positioning and resulted in less trauma to surrounding normal tissue. CT-guided <sup>125</sup>I particle interstitial implantation suppressed tumor growth and proliferation by regulating apoptotic-related genes and protein expression. This study provided an important basis and experimental foundation for the application of <sup>125</sup>I particle interstitial implantation in clinic.

## Conflict of interest

The authors declare no competing financial or commercial interests in this paper.

## References:

- Fujiki M, Aucejo F, Choi M, Kim R: Neo-adjuvant therapy for hepatocellular carcinoma before liver transplantation: Where do we stand? *World J Gastroenterol*, 2014; 20: 5308–19
- Silvestris N, Marech I, Brunetti AE et al: Predictive factors to targeted treatment in gastrointestinal carcinomas. *Cancer Biomark*, 2014; 14: 151–62
- Chvetsov AV, Yartsev S, Schwartz JL, Mayr N: Assessment of interpatient heterogeneity in tumor radiosensitivity for nonsmall cell lung cancer using tumor-volume variation data. *Med Phys*, 2014; 41: 064101
- Tishler RB: Increased clarity on the use of radiotherapy in the management of desmoplastic melanoma. *Cancer*, 2014; 120: 1315–18
- Huang J, Chunta JL, Amin M et al: Early treatment response monitoring using 2-deoxy-2-[<sup>18</sup>F]fluoro-D-glucose positron emission tomography imaging during fractionated radiotherapy of head neck cancer xenografts. *Biomed Res Int*, 2014; 2014: 598052
- Li L, Leung PS: Use of herbal medicines and natural products: An alternative approach to overcoming the apoptotic resistance of pancreatic cancer. *Int J Biochem Cell Biol*, 2014; 53: 224–36
- Quintas-Cardama A, Daver N, Kim H et al: A prognostic model of therapy-related myelodysplastic syndrome for predicting survival and transformation to acute myeloid leukemia. *Clin Lymphoma Myeloma Leuk*, 2014; 14: 401–10
- Leth T, von Oettingen G, Lassen-Ramshad YA et al: Survival and prognostic factors in patients treated with stereotactic radiotherapy for brain metastases. *Acta Oncol*, 2015; 54: 107–14
- Chen P WX, Liang WJ: Preliminary study of permanent <sup>103</sup>Pd radioactive seed implantation on malignant tumor in brachytherapy. *J Mod Clin Med Bioeng*, 2001; 7: 426–28
- Stankovic U, van Herk M, Ploeger LS, Sonke JJ: Improved image quality of cone beam CT scans for radiotherapy image guidance using fiber-inter-spaced antiscatter grid. *Med Phys*, 2014; 41: 061910
- Krishnan K, Liu J, Kohli K: Feature-space assessment of electrical impedance tomography coregistered with computed tomography in detecting multiple contrast targets. *Med Phys*, 2014; 41: 061903
- Connell T, Alexander A, Papaconstadopoulos P et al: Delivery validation of an automated modulated electron radiotherapy plan. *Med Phys*, 2014; 41: 061715
- Thapliyal A, Chandola-Saklani A, Bhatt D, Anhtwal P: Binding pattern of <sup>125</sup>Iodine thyroxine and tri-iodothyronine in skin and liver tissues of spotted munia, *Lonchura punctulata*: Co-relation to seasonal cycles of breeding and molting. *Indian J Exp Biol*, 2014; 52: 478–88
- Liu N, Liu S, Xiang C et al: Radioactive self-expanding stents give superior palliation in patients with unresectable cancer of the esophagus but should be used with caution if they have had prior radiotherapy. *Ann Thorac Surg*, 2014; 98: 521–26
- Sekiguchi A, Ishiyama H, Satoh T et al: <sup>125</sup>Iodine monotherapy for Japanese men with low- and intermediate-risk prostate cancer: Outcomes after 5 years of follow-up. *J Radiat Res*, 2014; 55: 328–33
- Li JR, Sun Y, Liu L: Radioactive seed implantation and lobaplatin chemotherapy are safe and effective in treating patients with advanced lung cancer. *Asian Pac J Cancer Prev*, 2015; 16: 4003–6
- Bize P, Duran R, Fuchs K et al: Antitumoral effect of sunitinib-eluting beads in the rabbit VX2 tumor model. *Radiology*, 2016; 26: 150361
- Beydoun N, Bucci J, Malouf D: Iodine-125 prostate seed brachytherapy in renal transplant recipients: An analysis of oncological outcomes and toxicity profile. *J Contemp Brachytherapy*, 2014; 6: 15–20
- Aoyagi K, Kouhiji K, Miyagi M et al: Expression of p27Kip1 protein in gastric carcinoma. *Hepatogastroenterology*, 2013; 60: 390–94
- Gryko M, Guzinska-Ustymowicz K, Kisluk J et al: High Fas expression in gastric carcinoma cells as a factor correlating with the occurrence of metastases to regional lymph nodes. *Adv Med Sci*, 2014; 59: 47–51
- Xu Y, He B, Li R et al: Association of the polymorphisms in the Fas/FasL promoter regions with cancer susceptibility: A systematic review and meta-analysis of 52 studies. *PLoS One*, 2014; 9: e90090
- Taira N, Kawabata T, Ichi T et al: Long-term survival after surgical treatment of metachronous bilateral adrenal metastases of non-small cell lung carcinoma. *Am J Case Rep*, 2014; 15: 444–46
- Gryko M, Pryczynicz A, Zareba K et al: The expression of Bcl-2 and BID in gastric cancer cells. *J Immunol Res*, 2014; 2014: 953203
- Yang Q, Shao Y, Shi J et al: Concomitant PIK3CA amplification and RASSF1A or PAX6 hypermethylation predict worse survival in gastric cancer. *Clin Biochem*, 2014; 47(1–2): 111–16

25. Zhao LW, Zhong XH, Yang SY et al: Inotodiol inhibits proliferation and induces apoptosis through modulating expression of cyclinE, p27, bcl-2, and bax in human cervical cancer HeLa cells. *Asian Pac J Cancer Prev*, 2014; 15: 3195–99
26. Chaturvedi R, Asim M, Piazzuelo MB et al: Activation of EGFR and ERBB2 by *Helicobacter pylori* results in survival of gastric epithelial cells with DNA damage. *Gastroenterology*, 2014; 146: 1739–51e1714
27. An X, Wang F, Shao Q et al: MET amplification is not rare and predicts unfavorable clinical outcomes in patients with recurrent/metastatic gastric cancer after chemotherapy. *Cancer*, 2014; 120: 675–82